SOILS AND FOUNDATIONS Vol. 46, No. 2, 233–245, Apr. 2006
Japanese Geotechnical Society

CYCLIC RESISTANCE OF CLEAN SAND IMPROVED BY SILICATE-BASED PERMEATION GROUTING

YOSHIMICHI TSUKAMOTO[i], KENJI ISHIHARA[ii], KEITARO UMEDA[iii] and TADAO ENOMOTO[iv]

ABSTRACT

The cyclic resistance of clean sand improved by silicate-based permeation grouting is examined based on laboratory triaxial tests. Specimens were prepared by the methods of sedimentation and wet tamping. In the former method, dry sand was poured into the silicate-based solution. In the latter method, grouting was conducted by permeating silicate-based solution through wet-tamped nearly-dry specimens as well as through wet-tamped nearly-saturated sand specimens. The overburden stress was applied on some of the grouted saturated sand specimens during a curing period typically of one month. For all of the specimens prepared in different ways as above, the non-destructive measurements were first conducted of velocities of P-wave and S-wave propagation through the samples prepared under varying *B*-values. The aim of these measurements was to examine whether the small-strain properties of grouted sand specimens with gelled soil fabrics can be evaluated in the general framework of the theory of poro-elasticity. The undrained cyclic triaxial test was then conducted on each of the specimens. The influence of grouting on dry sand and saturated sand, and the effects of sustained application of an overburden stress during the curing period were examined drawing attention to the inner structure of grouted sand and its effects on the cyclic resistance.

Key words: cyclic resistance, permeation grouting, sand (**IGC**: D6/D7)

INTRODUCTION

Permeation grouting has been developed for improving sand deposits as one of countermeasures against soil liquefaction during earthquakes. Among various other alternatives, this technique has an advantage in that it can be implemented even under difficult site conditions such as reinforcing loose sand deposits under existing airport runways or around existing bridge piers. Application of this technique is also being explored in order to improve loose sands underneath storage tanks so as to make them more resistant to liquefaction. In the permeation grouting, the specially prescribed silicate-based (SiO_2) solution is used, which is produced by extracting alkali substances from water glass and therefore environmentally harmless. This solution is initially permeable enough to travel through soil aggregates and to gradually solidify into gel-like formation.

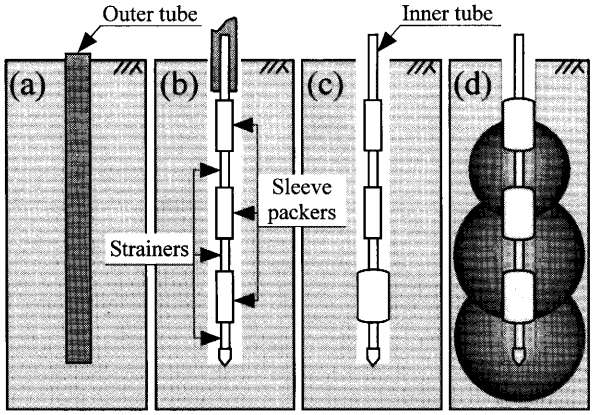

(a) Insert an outer tube.
(b) Insert an inner tube and pull out the outer tube.
(c) Inflate sleeve packers from bottom.
(d) Inject silicate-based solution from strainers.

Fig. 1. Operational procedure of permeation grouting

In the typical practice of permeation grouting used in Japan, a main tube consisting of inner and outer tubes, equipped with packers and strainers, is lowered into the bored hole, as shown in Fig. 1. The strainers are fixed at three locations each about 15 cm apart along the surface of the main tube for ejecting the silicate solution through the inner tube encased in the main tube. In between the two neighboring strainers, rubber-sleeved packers are fixed which can be expanded radically by pressurized water from the outer tube encased in the main tube. In its operation the rubber sleeves are first inflated within the borehole by sending pressurized water through the outer

[i] Associate Professor, Department of Civil Engineering, Tokyo University of Science, Japan (ytsoil@rs.noda.tus.ac.jp).
[ii] Professor, ditto.
[iii] Kyowa Exeo Corporation, Japan (formerly Graduate Student, ditto).
[iv] Graduate Student, ditto.
The manuscript for this paper was received for review on September 8, 2005; approved on January 13, 2006.
Written discussions on this paper should be submitted before November 1, 2006 to the Japanese Geotechnical Society, 4-38-2, Sengoku, Bunkyo-ku, Tokyo 112-0011, Japan. Upon request the closing date may be extended one month.

tube, thereby isolating the soil mass to be grouted. Then, the silicate solution is ejected through the inner tube to push silicate liquid outwards from the strainers into the surrounding sand deposits. By this operation, the silicate liquid is forced to permeate into a spherical soil zone with its centre located at the mouth of the strainer. After a curing period of about one month, a chain of sphere-shaped solidified zone is formed in the vertical alignment for one borehole. By carrying out the same operation at other neighboring boreholes, the targeted zone of loose sand deposits can be grouted and solidified. This method is conceived as applicable to layers of sandy soils with fines content less than 35% located down as deep as 20 metres below the ground surface.

There are past studies addressing chemical grouting in Japan (Mori et al., 1989; Hatanaka et al., 2002 and others), which has been used widely to create impermeable layers within grounds and to stabilize soil masses during underground excavation. Mori and Tamura (1986) addressed the permeability of sands stabilized by water glass-based chemical grouting, which was shown to be changing with shear deformation and was examined with reference to dilatancy characteristics of sands. Kaga and Yonekura (1991) examined extensively the unconfined compression strength of chemically grouted sands with a wide range of properties.

In order to clarify basic physical characteristics of the sand solidified as above, a series of laboratory tests were conducted on silicate-grouted sand specimens prepared by different methods with or without surcharge being applied during the curing period. In the laboratory triaxial samples, the small strain was applied first in non-destructive manner to monitor shear and compressive wave velocities, and then cyclic shear stress was applied to evaluate the cyclic resistance. The outcome of these studies will be described in the following pages of this paper.

MATERIAL AND SAMPLE PREPARATION

Four methods were employed in this study for preparing specimens for the cyclic triaxial tests, as illustrated in Fig. 2. The variation as such in the method of sample preparations was intended to examine whether the cyclic resistance of solidified sand is affected by the characteristics of fabric structures produced by different methods of preparation. It was also intended to clarify whether the sustained application of an overburden stress during the curing period may or may not exert any influence on the mode of formation of gelled substances (gel-formation) within soil fabrics and further on the cyclic resistance of soils.

The grouting material used in the present study is the specially prescribed silicate-based (SiO_2) solution, which is produced by extracting alkali substances from water glass using electro-osmosis. The typical gel time of this material is about a couple of ten minutes to hours.

In all series of the tests, soil specimens 60 mm in diameter and 120 mm in height were prepared using Toyoura sand. This sand is classified as poorly graded clean fine sand with no fines, and its specific gravity is $G_s = 2.66$ with a mean particle diameter $D_{50} = 0.18$ mm. The maximum and minimum void ratios are $e_{max} = 0.973$ and $e_{min} = 0.607$, respectively. The methods of sample preparation employed were as follows.

Test Series O

In the test series O, samples were saturated with water alone and silicate-based solution was not used. Sand specimens were prepared by the method of air pluviation (A.P.), wet tamping (W.T.) and water sedimentation (W.S.). They were then nearly saturated by circulating water and by controlling the back pressure for varying levels of the *B*-value and tested in the triaxial test apparatus.

Test Series A

In this test series, dry sand was poured into the mould filled with liquid of the silicate-based solution and made to sediment to form specimens for triaxial testing. The water used contained 6% liquid silicate. The silicate content of 6% was the minimum to form specimens competent enough to stand by self-weight. If the silicate content is below 6%, it was not possible to form a specimen. With this method of sedimentation, it was difficult to precisely attain targeted values of the relative density. Thus, specimens were prepared so as to attain a given range of the relative density, as accordingly shown in Table 1. No overburden stress was applied on the specimens during the curing period of about one month.

Test Series B

In this test series, dry sand was first mixed to attain 5% water content. The water used here contained 6% liquid silicate. The moist sand thus prepared was tamped uniformly in several layers within the mould to achieve the relative densities of $D_r = 25$, 40 and 55%. After removing the mould the specimen was made to stand by vacuum in the triaxial cell, and then, the silicate solution was circulated through the specimen and it was left at rest for being cured for a period of about one month. With this procedure, it was found that approximately 75% of void in volume was saturated with the liquid of silicate solution with the remaining 25% occupied by pore air. The characteristics of the test series were that the specimens were permeated by the silicate solution through nearly dry sand, but with no overburden pressure applied during the curing period as accordingly indicated in Table 1.

Test Series C

In this test series, moist sand with about 5% water content without silicate was tamped uniformly in several layers within the mould, and deaired water was circulated through the specimens to make them almost fully saturated with water. Similar to the test series B, the specimens with the relative densities of $D_r = 25\%$ and 40% were prepared. From this stage onwards, the silicate solution of 6% was permeated through the specimen. The

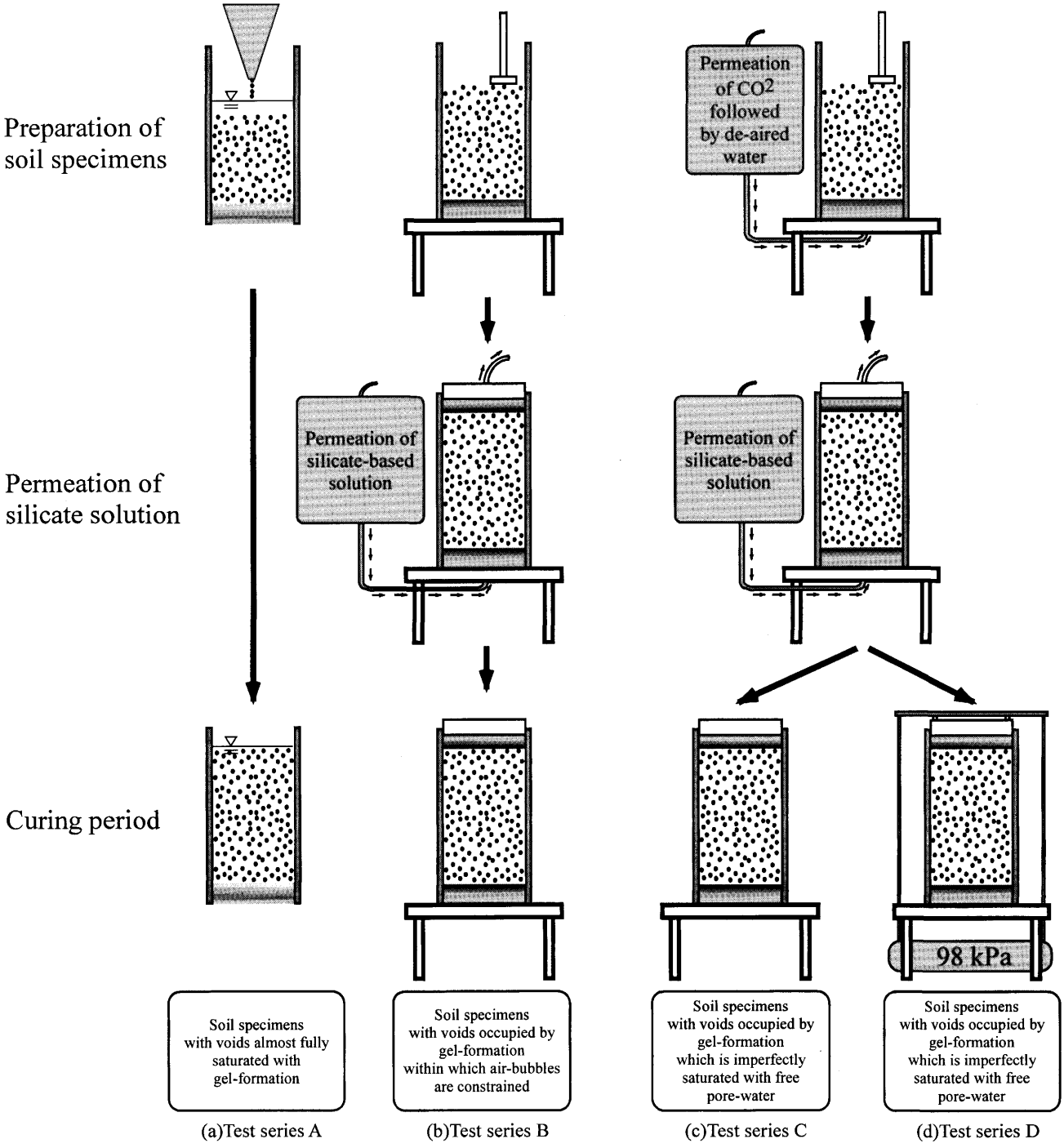

Fig. 2. Preparation of soil specimens and test series

specimen was then cured for a period of about one month without applying the surcharge. The particular feature of this test series was that the specimens were permeated with deaired water first for full saturation, and were then grouted or permeated by the silicate solution, as indicated in Table 1. No overburden pressure was applied during the curing period.

Test Series D

In this test series, the specimens were prepared in the same manner as in the test series C by employing the grouting through water-saturated sand. The intention of this test series was to see the effect of overburden during the curing period. Thus, the specimens were subjected to the sustained application of an overburden stress of 98 kPa over the one-month period of curing.

TESTING PROCEDURES

The testing scheme was the same as that previously used and described in detail by Tsukamoto et al. (2002), Nakazawa et al. (2004) and Ishihara and Tsukamoto

Table 1. Test series and summary of response during measurements of *B*-value, P-wave and S-wave velocities

Test series	D_r (%)	Preparation method	Silicate-based grouting conducted	Overburden stress	Range of observed *B*-value	Type of V_p-response	Number of specimens
O	40 & 60	A.P.	No grouting	No	0 ~ 1.0	Type-A: V_p changes with *B*-value	
	25 & 40	W.T.					
	40 & 55	W.S.					
A	20 ~ 30	Sedimentation into silicate solution		No	0.1 ~ 0.8	Type-B: V_p stays around 1650 m/s	6
	35 ~ 45						5
	50 ~ 60						6
B	25	W.T.	Grouting through dry sand	No	0 ~ 0.45	Type-A	7
	40						6
	55						6
C	25		Grouting through water-saturated sand	No	0 ~ 1.0	Type-B	10
	40						9
D	25			Yes		Type-A	3
						Type-B	3
	40					Type-A	1
						Type-B	5

(1) In the preparation method, A.P., W.T. and W.S. stand for air pluviation, wet tamping and water sedimentation, respectively.
(2) Overburden stress indicates whether the sustained application of an overburden stress was made during the curing period.
(3) Type of V_p-response: Type-A corresponds to the response where the velocity of P-wave changes with the *B*-value in accordance with the theoretical expression (2). Type-B corresponds to the response where the velocity of P-wave stays constant around $V_p = 1650$ m/s irrespective of the *B*-value.

(2004). Figure 3 shows the cross section of a soil sample 60 mm in diameter and 120 mm in height, which is placed between the cap and pedestal equipped with the transducers for P-wave and S-wave velocity measurements. The transducer working as a source of P-wave generation is a piezo-electrically driven bolt-clamped ceramic transducer, whereas the transducer for a receiver of P-wave propagation is a piezo-electric accelerometer, which is attached to a dummy metal block plugged into the pedestal. A pair of bender elements was installed at the cap and pedestal as a source and a receiver of S-wave propagation, respectively, travelling through the triaxial specimen. The velocities of P-wave and S-wave propagation could be obtained by monitoring the difference in time between dispatch and arrival.

The tests consisted of two phases, which are the non-destructive test monitoring the velocities of shear wave V_s and longitudinal wave V_p, and the destructive test where cyclic stress was applied undrained leading to large shear strains near failure. After finishing the series of procedures of sample preparation, the specimen was first isotropically consolidated to a given confining stress σ'_0, and the *B*-value was measured. The non-destructive test was then conducted monitoring the velocities of shear wave V_s and longitudinal wave V_p under given *B*-values. Herein, in order to achieve a targeted *B*-value, the back pressure was controlled while the effective confining stress was maintained constant. In the undrained cyclic triaxial test conducted afterwards, the *B*-value was increased to the highest value achievable in the specimen. The specimen was then put under the p-constant condition. In other words, the lateral stress was reduced while the axial stress was increased and vice versa in the cyclic phase of load application to maintain the change in the mean principal stress equal to zero, $\Delta p = (\Delta\sigma_1 + 2\Delta\sigma_3)/3 = 0$. The cyclic stress ratio, $\sigma_d/(2\sigma'_0)$, was applied undrained with a frequency of 0.1 Hz. The p-constant —condition was considered important particularly in the loading tests on partly saturated samples. This aspect was addressed in the previous paper by Tsukamoto et al. (2002).

MEASUREMENT AND ANALYSIS OF V_p AND V_s

The velocities of P-wave and S-wave propagation were measured under varying *B*-values. This testing method was found to be useful in inferring the basic small-strain properties of soils, based on the theory of poro-elasticity. The two parameters of the shear modulus G_0 and Poisson's ratio ν at small strains are one of the combinations for determining the elastic material properties. The shear modulus G_0 can be calculated solely from the velocity of S-wave propagation with the simple expression of $G_0 = \rho V_s^2$, and has been found to be independent of the *B*-value as shown in the following section. On the other hand, based on the theory of wave propagation through a porous medium by Kokusho (2000) and Tsukamoto et al. (2002), the overall Poisson's ratio ν is expressed as

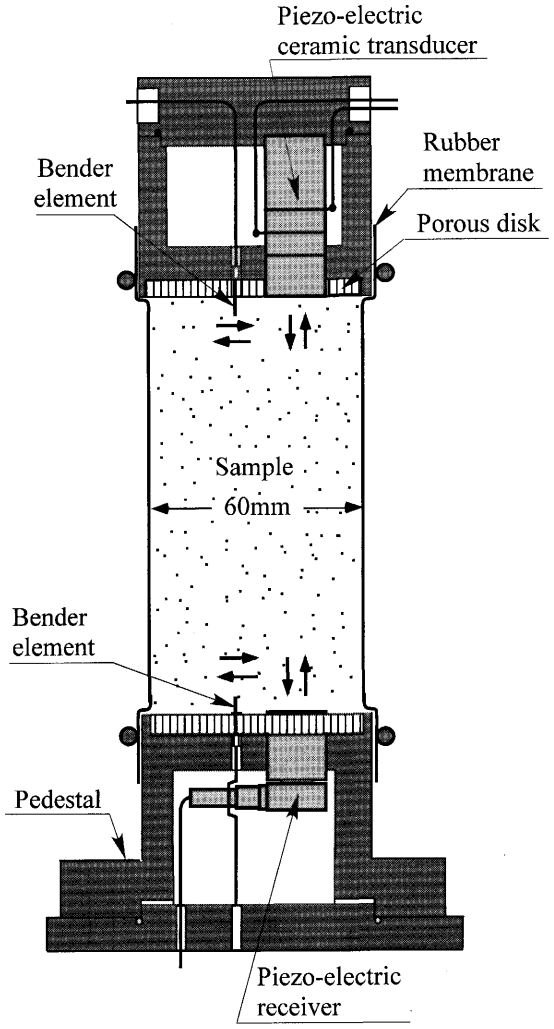

Fig. 3. Cross sections of the cap, samples and pedestal with transducers (after Tsukamoto et al., 2002)

function of the B-value in the following form,

$$v=\frac{(V_p/V_s)^2-2}{2(V_p/V_s)^2-2}=\frac{3\nu_b+(1-2\nu_b)B}{3-(1-2\nu_b)B}, \quad (1)$$

where ν_b is the skeleton Poisson's ratio pertaining to the skeleton deformation of the medium. Note that the overall Poisson's ratio, v, is associated with the deformation of the skeleton and pore water. In other words, v pertains to the undrained deformation. It is also possible to infer the value of ν_b by inspecting the relation of V_p/V_s against the B-value obtained from the series of tests with reference to the expression as follows,

$$(V_p/V_s)^2=\frac{4}{3}+\frac{2(1+\nu_b)}{3-(1-2\nu_b)(1-B)}. \quad (2)$$

In what follows, the relation of V_p and V_s against the B-value is adopted in presenting the data of the tests. Figure 4(a) shows the results of the test series O in terms of the plot of the B-value against the velocities of P-wave and S-wave propagation, V_p and V_s, for the case of non-grouted Toyoura sand with the relative density of $D_r=30\%$. The plots of the B-value against the overall Poisson's ratio, v, are also shown in Fig. 4(b). The simi-

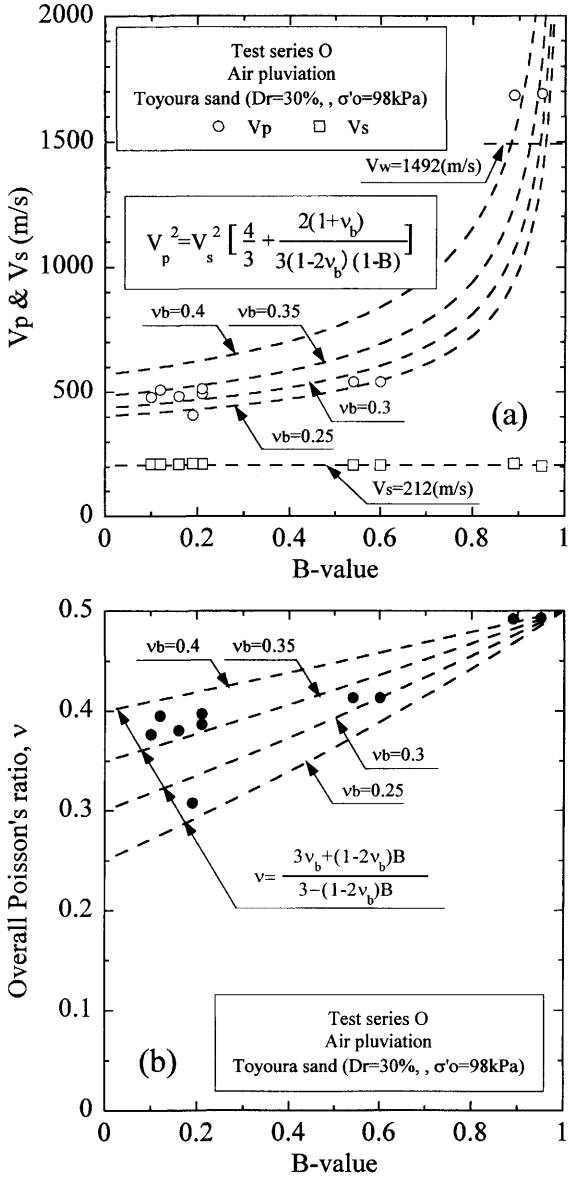

Fig. 4. Results of non-destructive tests in test series O ($D_r=30\%$): (a) V_p & V_s against B-value and (b) overall Poisson's ratio against B-value

lar set of data for the relative density of $D_r=40\%$ is shown in Figs. 5(a) and (b). These test results were presented in the previous paper by Tsukamoto et al. (2002). When the soil is fully saturated, the velocity of P-wave takes a value slightly greater than the value for the compressional wave through water. By examining the plots in Figs. 4 and 5 with reference to the theoretical relationship of Eq. (2), it may be reasonable to assume that the skeleton Poisson's ratio ν_b takes a value of about 0.35 for Toyoura sand.

Figures 6(a) and (b) show the plots of the B-value against V_p and V_s as well as v, obtained from the test series A with $D_r=20$–30%. Another set of data for the test series A for the relative density of $D_r=35$–45% is shown in Figs. 7(a) and (b). In these series of tests, specimens were prepared by pouring the dry sand into the silicate-based solution, and without further permeation

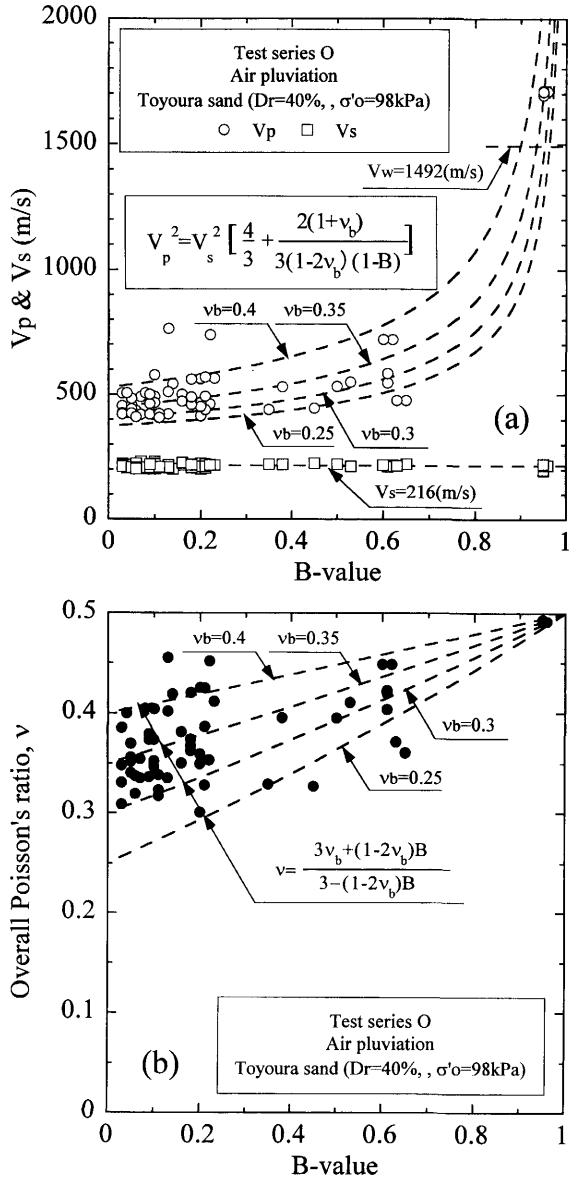

Fig. 5. Results of non-destructive tests in test series O (D_r=40%): (a) V_p & V_s against B-value and (b) overall Poisson's ratio against B-value

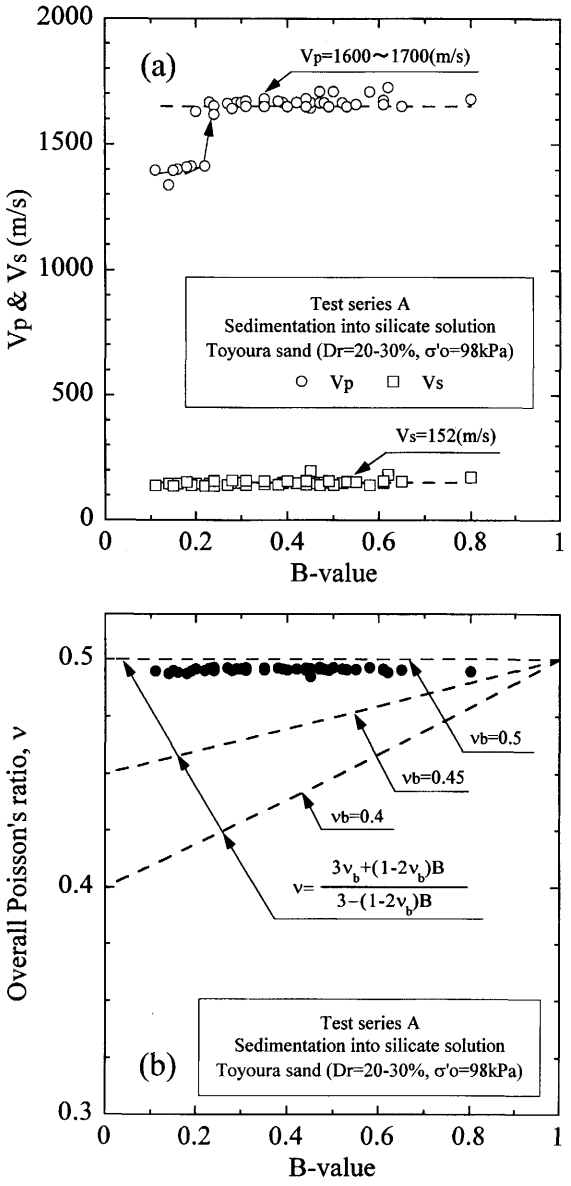

Fig. 6. Results of non-destructive tests in test series A (D_r=20–30%): (a) V_p & V_s against B-value and (b) overall Poisson's ratio against B-value

or grouting of the silicate solution, the specimens were kept under an atmospheric pressure during the curing period. The results of the tests show the value of V_s= 152 m/s and 171 m/s for the relative densities of D_r= 20–30% and 35–45%, respectively. Similar to the case of water-saturated sand shown in Figs. 4(a) and 5(a), the velocity of S-wave propagation, V_s, for the silicate-sedimented sand is shown also to stay constant regardless of the B-value, as shown in the plots of Figs. 6(a) and 7(a). It is easy to understand that the shear wave effectively propagates through fabrics of soil aggregates, and its velocity is independent of whether the void is saturated with water or occupied by gelled substance. However, the velocity of P-wave propagation, V_p, appears to be constant at about V_p=1650 m/s regardless of the B-value, except for some of the test specimens which follow the theoretical relation of Eq. (2) assuming ν_b=0.487. It is highly likely that, in the case of the silicate-sedimented sand with enough liquid, well-developed structures of gelled substance prevailed within fabrics of sand particles, through which the wave may travel primarily without interaction with pore water. Therefore, the value of V_p became constant at about 1650 m/s.

Figures 8(a) and (b) show the plots of the B-value against V_p and V_s as well as ν, obtained from the test series B with D_r=25%. The set of data prepared by the same method is shown in Figs. 9(a) and (b), for the case of the relative density of D_r=40%. In these series of tests, silicate-based permeation or grouting was performed on wet-tamped nearly dry sand specimens with the relative densities of D_r=25% and 40%, and the soil specimens were kept under an atmospheric pressure with no surcharge during the curing period. It is seen in Figs. 8 and 9 that the B-value ranges between 0 and 0.45, and

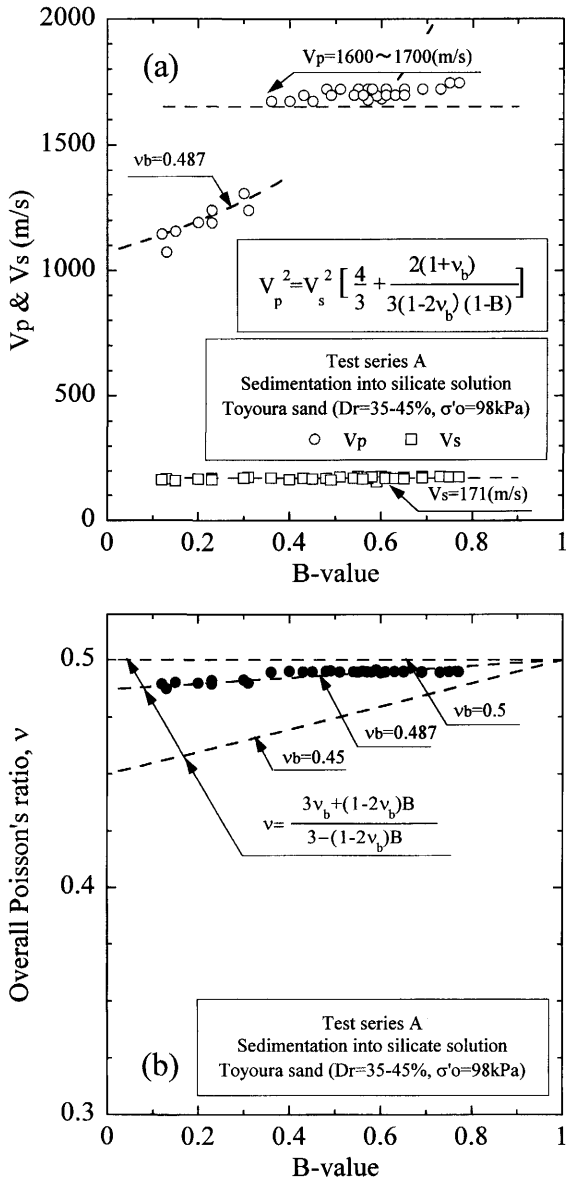

Fig. 7. Results of non-destructive tests in test series A (D_r=35–45%): (a) V_p & V_s against B-value and (b) overall Poisson's ratio against B-value

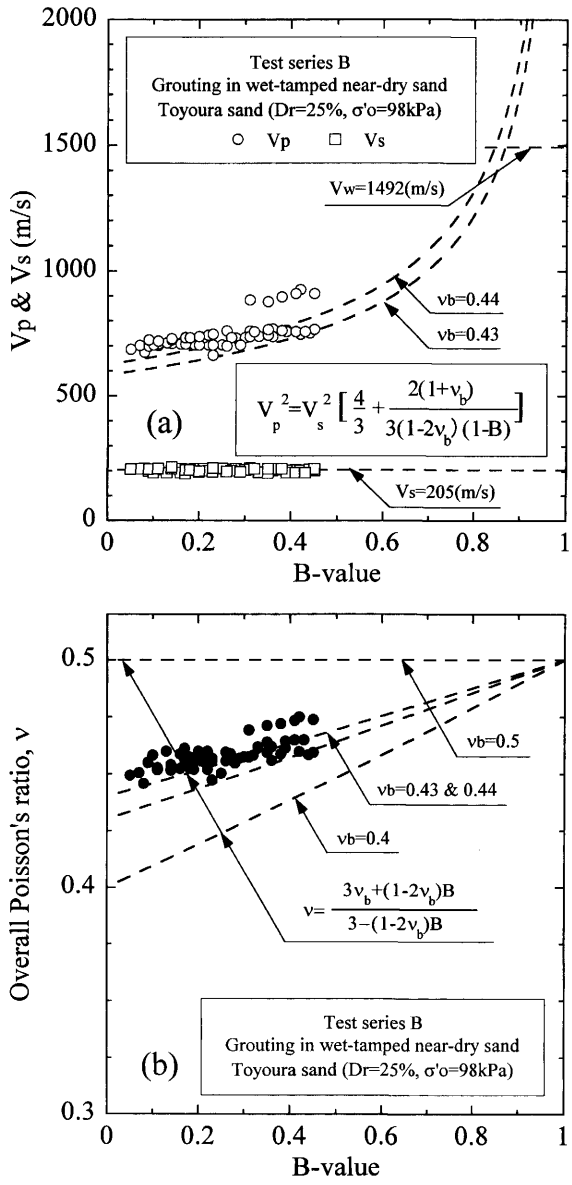

Fig. 8. Results of non-destructive tests in test series B (D_r=25%): (a) V_p & V_s against B-value and (b) overall Poisson's ratio against B-value

does not go up beyond 0.45, because of the dry nature of the samples. It may be seen also that the value of V_p approximately follows the theoretically derived curves assuming the values of about ν_b=0.43 to 0.44. Since the B-value is the pore pressure response during undrained isotropic compression, it can be said that the B-value of the specimens prepared as above is incapable of rising above the value of 0.45, due to a fairly large amount of air bubbles entrapped within the voids. The primary wave is therefore thought to propagate through the solidified structure of gelled substance with trapped pore air bubbles, and the skeleton Poisson's ratio of such inner structures takes a value of ν_b=0.43 to 0.44.

Figures 10(a) and (b) show the plots of the B-value against V_p and V_s as well as ν_b, obtained from the test series C with a relative density of D_r=25%. The same set of data for the relative density of D_r=40% is shown in Figs. 11(a) and (b). In these series of tests, silicate-based permeation was performed on wet-tamped nearly saturated sand specimens with the relative densities of D_r=25 % and 40%, and the soil specimens were kept under an atmospheric pressure without surcharge during the curing period. It may be seen that the value of V_p stays constant at about 1650 m/s, and is independent of the B-value. From this observation, it can be said that there seem to be well-developed solidified structures of gelled substance occupying the voids continuously from the bottom to the top of the soil specimens, through which the primary wave was transmitted. On the other hand, the B-value ranges fully from 0 to 1. This may be due to the fact that the structure of gelled substance was existent together with partly saturated water, and the latter must have acted independently as a medium to respond to pore pressure gauge, producing various B-values. In fact,

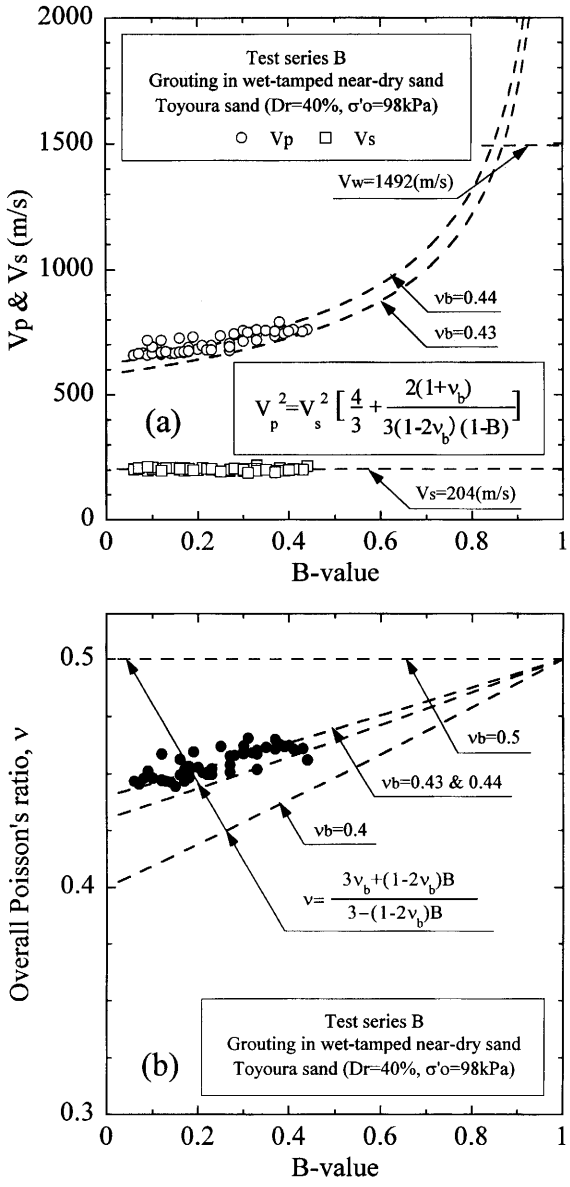

Fig. 9. Results of non-destructive tests in test series B ($D_r = 40\%$): (a) V_p & V_s against B-value and (b) overall Poisson's ratio against B-value

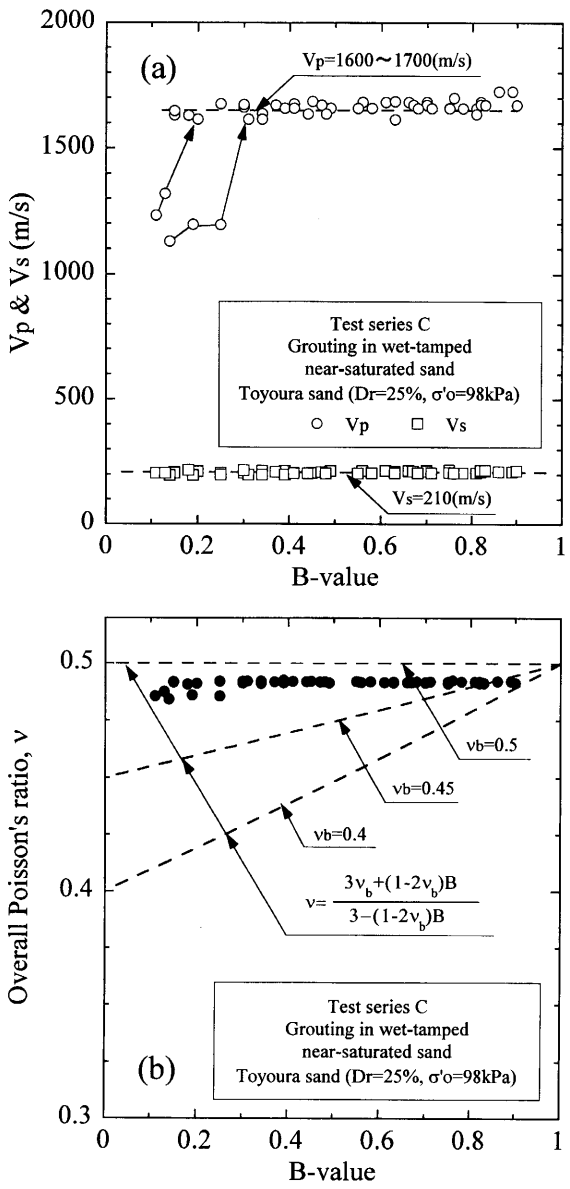

Fig. 10. Results of non-destructive tests in test series C ($D_r = 25\%$): (a) V_p & V_s against B-value and (b) overall Poisson's ratio against B-value

without any interaction with the air in the pores, through the continuous path formed by the gelled substance, the primary wave seems to have propagated.

Figures 12(a) and (b) show the plots of the B-value against V_p and V_s as well as ν_b, obtained from the test series D with a relative density of $D_r = 25\%$. The same set of data for the relative density of $D_r = 40\%$ is shown in Figs. 13(a) and (b). In these series of tests, silicate-based grouting was conducted on wet-tamped nearly saturated sand specimens and they were subjected to the sustained application of an overburden stress of 98 kPa over the curing period of about one month. Although each specimen was prepared under the identical procedures, there were two different types of response that were observed in each of this test series. In each type, the shear wave response was the same, with a value of $V_s = 209$ m/s for $D_r = 25\%$ and a value of $V_s = 220$ m/s for $D_r = 40\%$. The main difference appeared in the P-wave response as classified as below.

Type-A Response:

P-wave velocity changes with the B-value, which is similar to those observed in the test series O and B, where there was no grouting or grouting into nearly dry sand.

Type-B Response:

P-wave velocity stays constant at about $V_p = 1650$ m/s, and is independent of the B-value, which is the response similar to that observed in the test series A and C, where there were abundance of water and silicate at the time of the sample preparation.

The difference in the observed response between Type-A and Type-B is illustrated in Fig. 14. It is to be mentioned that there is no definite reason accountable for a

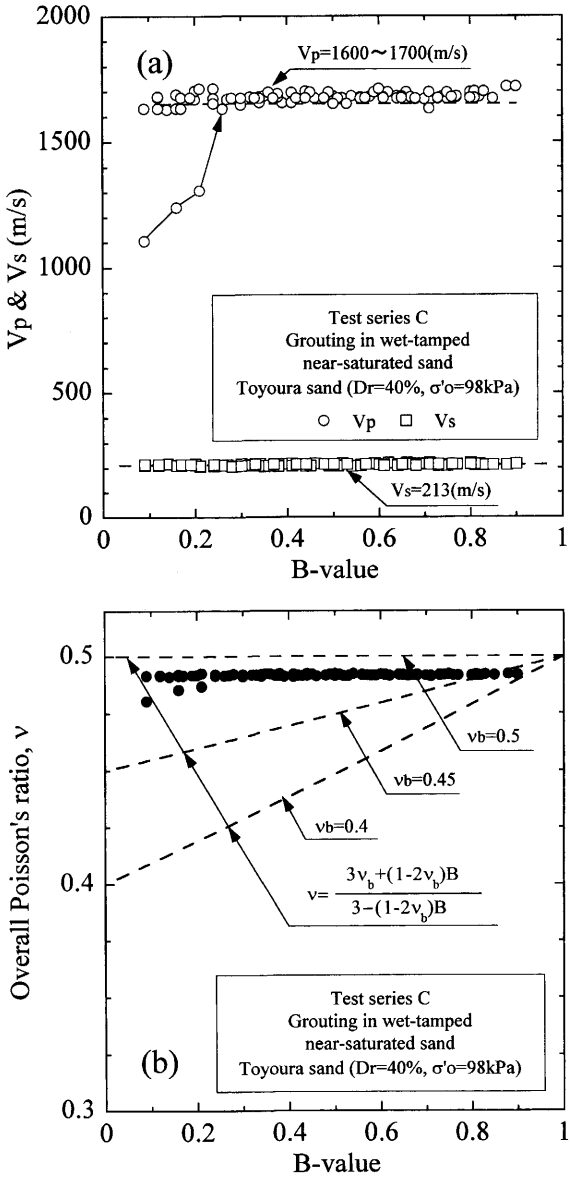

Fig. 11. Results of non-destructive tests in test series C ($D_r = 40\%$): (a) V_p & V_s against B-value and (b) overall Poisson's ratio against B-value

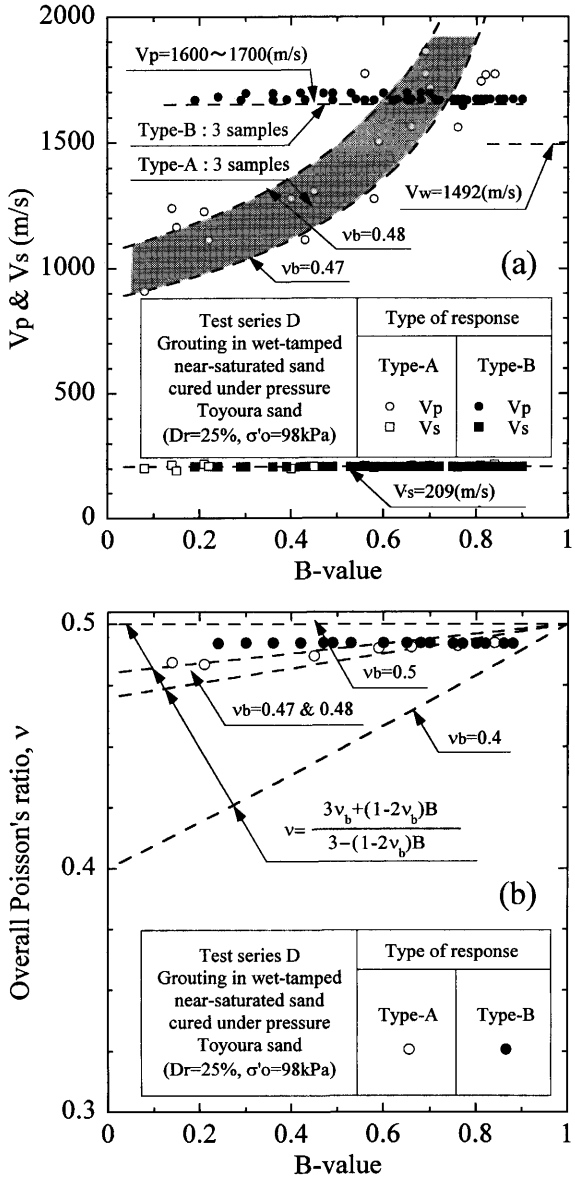

Fig. 12. Results of non-destructive tests in test series D ($D_r = 25\%$): (a) V_p & V_s against B-value and (b) overall Poisson's ratio against B-value

given sample to distinguish whether it will exhibit Type-A or Type-B response. A conceivable scenario in explaining the two different types of response would be that in some of the soil specimens, the structures of gelled substance developed during the curing period were destroyed and fractured due to the sustained application of an overburden stress, and the fractured structure was filled with imperfectly saturated free water, thus showing the response of Type-A, where the V_p-value changed with the B-value. On the other hand, the other specimens were exempted from such fracture and showed the response of Type-B keeping the V_p-value unchanged, where the gelled substance remained intact acting as the continuous pathway for the P-wave propagation. It is to be noticed that for the specimens showing the response of Type-A, the skeleton Poisson's ratio was as high as $\nu_b = 0.46$ to 0.48. The summary of the observations distinguishing between Type-A and Type-B is presented in Table 1.

Various types of behaviour of sand samples prepared by different procedures are summed up, as shown in Fig. 14, in the form of a schematic diagram illustrating the relations between the P-wave velocity and the B-value observed in all of the test series employed in this study. Looking over at the diagram, one can initially notice that the P-wave velocity of non-grouted normal sand is lowest over all the B-values. The value of V_p is seen tending to increase if the sand is improved by silicate inclusion in any way. When there are bubbles in the pores in the gel-formation, the V_p-value tends to increase from 600 m/s upwards. If the gel-formation due to silicate is fractured, the P-wave velocity is seen rising further up. Eventually when the gel-formation is not destroyed, the value of V_p takes the highest value of about 1650 m/s irrespective of the B-value. It is also of interest to note

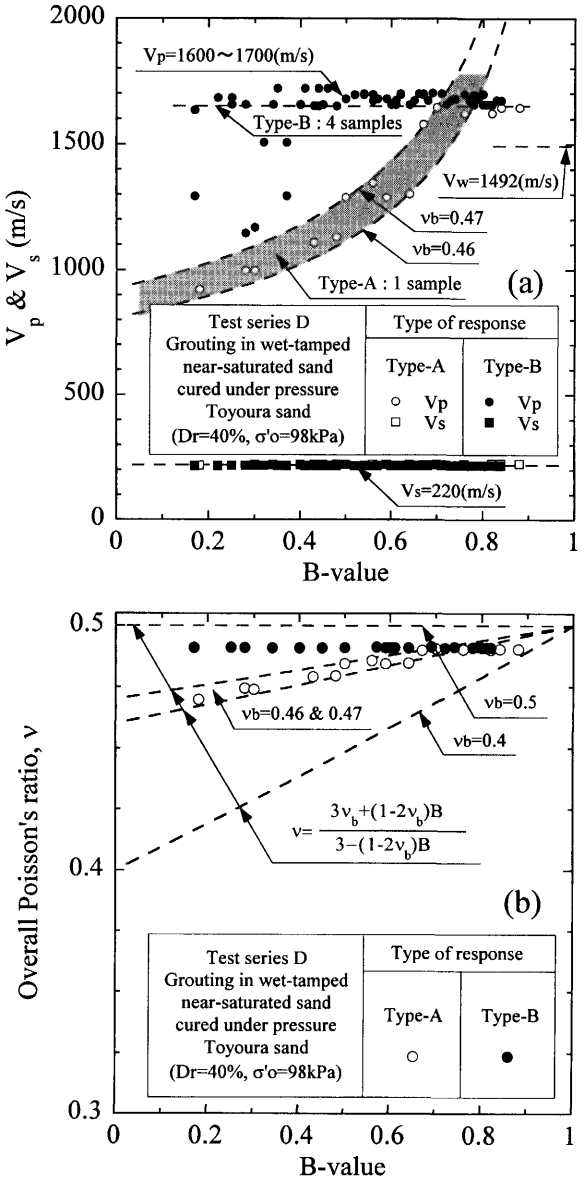

Fig. 13. Results of non-destructive tests in test series D ($D_r = 40\%$): (a) V_p & V_s against B-value and (b) overall Poisson's ratio against B-value

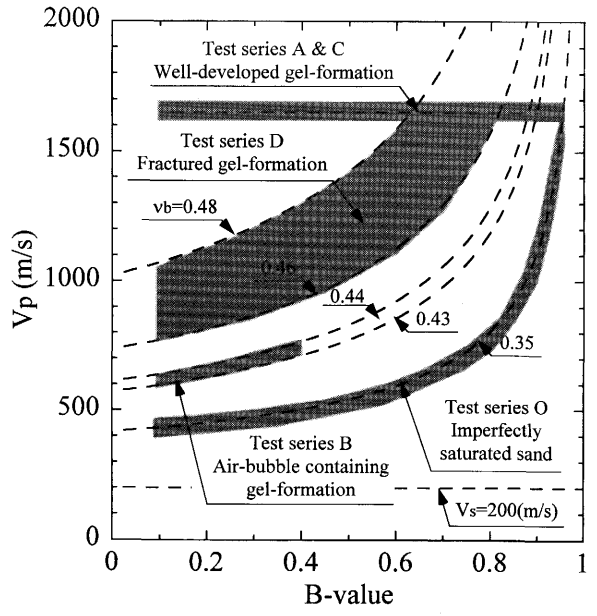

Fig. 14. Summary of the relations of V_p and V_s against B-value

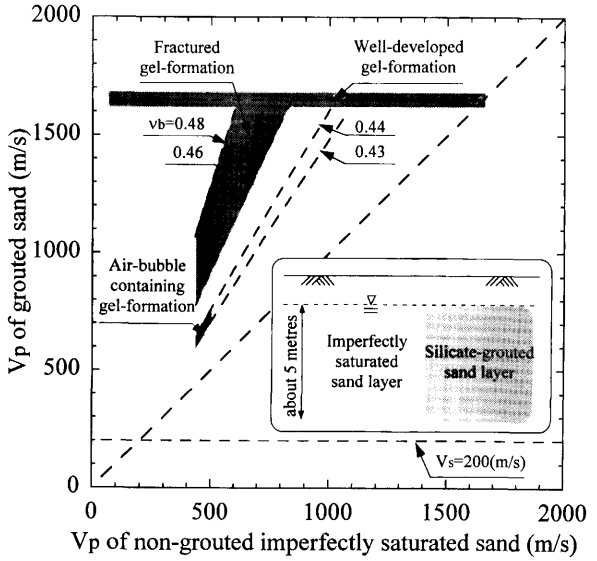

Fig. 15. Relation between velocities of P-wave propagation through imperfectly saturated sand and silicate-grouted sand

that the limiting value of V_p near $B=0$ takes a value of about 400 m/s for non-grouted sand with $\nu_b = 0.35$. This V_p-value becomes about 600 m/s with $\nu_b = 0.43$ for the samples containing air bubble in the geo-formation. For the grouted samples with fractured gel-formation, the V_p-value at $B=0$ is higher up in the range of 700–1000 m/s with $\nu_b = 0.46 \sim 0.48$. For the specimens having well-developed gel-formation, the value of V_p takes the highest value of 1650 m/s with the skeleton Poisson's ratio of $\nu_b \cong 0.50$.

In the practice of in-situ soil improvements, it is generally known (Ishihara et al., 2004), that imperfectly saturated soil layers often prevail down to a depth of about 5 metres below the groundwater level, and these layers are usually a target of ground improvement by means of silicate-based grouting. Therefore, it would be of interest to provide a diagram in which the P-wave velocity of non-grouted sand is plotted against the P-wave velocity of the sand grouted under varying conditions. Such a diagram can be provided with reference to the diagram in Fig. 14, with the result shown in Fig. 15. It is assumed here that the value of $V_s = 200$ m/s and $\nu_b = 0.35$ are taken for non-grouted sand. It may be seen that the P-wave velocity of grouted sand is always greater than that of non-grouted sand, but it may change depending upon the conditions under which the grouting is conducted in-situ producing different gel-formations within the pores in sand deposits.

In the technical report published by the technical committee of the Japanese Geotechnical Society (JGS, 1993), there are many methods recommended to evaluate

the field performance of chemical grouting, including standard penetration tests, dynamic cone penetration tests and laboratory triaxial tests. Other field exploration techniques are also recommended, including electrical resistivity method, electrical logging, velocity logging and others. Based on the chart shown in Fig. 15, correlating the propagation velocities of primary waves through non-grouted sand and grouted sand, it would be possible to refine the procedure of evaluating field performance of chemical grouting through velocity logging tests as follows. Since it was found from the present study that there is no change in the velocity of shear waves V_s induced by permeation grouting, the velocity of primary waves V_p is only used. In doing so, the results of two independent velocity logging tests are necessary. One of them needs to be conducted at a site located within a zone of chemically grouted areas. The other needs to be conducted at a site located outside of the chemically grouted areas. Since the soil layers located just beneath a groundwater level are known to be in partially saturated conditions and those layers are usually targets of permeation grouting, the velocity of primary waves V_p measured at a given depth at a site of non-grouted areas would indicate values less than 1500 m/s, which corresponds to a fully saturated condition. On the other hand, when the permeation grouting is performed successfully and the gelled soil structures are well developed within grounds, the value of V_p measured at a site of grouted areas would become close to about 1650 m/s. When the gelled soil structures suffer from any fracturing during the process of grouting and the subsequent curing periods, the value of V_p would be likely to stay lower in a range between 800 and 1650 m/s, however, it would still be greater than the counterpart of the V_p-value measured at the same depth at a site of non-grouted areas, as implied in Fig. 15. The interpretation of the data of velocity logging tests thus described would serve as a refined procedure for evaluating the performance of permeation grouting with good engineering judgement.

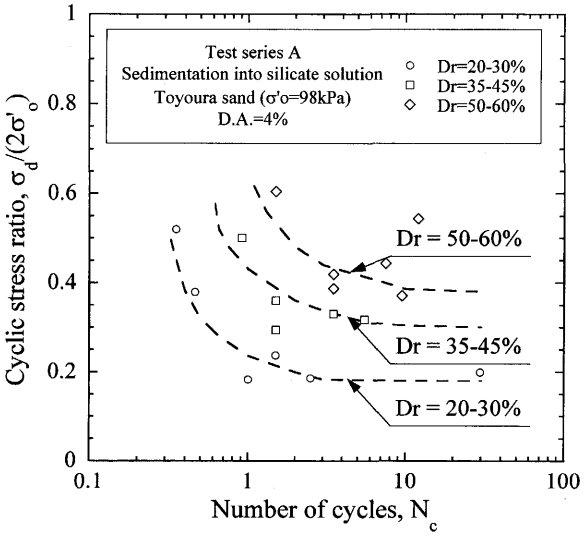

Fig. 16. Plots of cyclic stress ratio against number of cycles in test series A

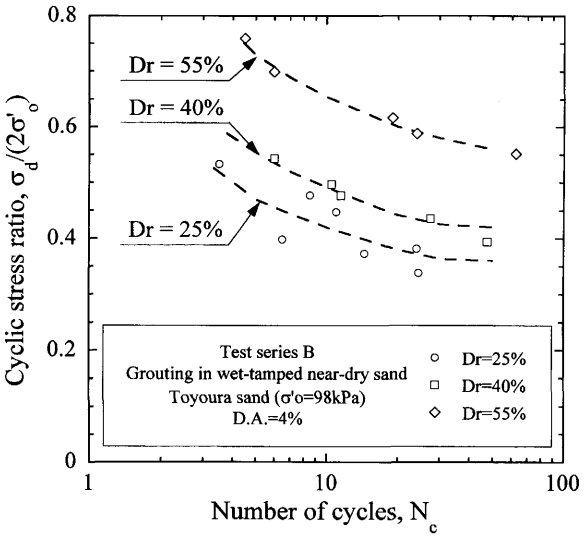

Fig. 17. Plots of cyclic stress ratio against number of cycles in test series B

CYCLIC TRIAXIAL TEST RESULTS

After non-destructive measurements of the velocities of P-wave and S-wave propagation, the undrained cyclic triaxial tests were conducted on the identical specimens.

Cyclic Stress Ratio against Number of Cycles

The data of undrained cyclic triaxial tests are summarized in the form of cyclic stress ratio $\sigma_d/(2\sigma_0')$ producing 4% double amplitude (DA) axial strain plotted against the number of cycles, N_c. In the usual practice, the DA axial strain amplitude of 5% is taken in such plots, but in the case of silicate-strengthened sand, some of the cyclic tests did not produce the DA axial strain of 5%. Thus, the 4% DA axial strain was considered appropriate as an index indicative of cyclic strength of the sand strengthened by addition of silicate.

The cyclic stress ratio causing the 4% DA amplitude axial strain in the test series A and B is plotted in Figs. 16 and 17 versus the number of cycles. It is seen that the cyclic strength defined above is highly dependent on the density. The data for the test series C and D are shown in Fig. 18. The relation is also found to be density-dependent.

From the observation of the non-destructive test results measuring the *B*-value, P-wave and S-wave velocities, it was found that the soil specimens of the test series B contained a sufficient amount of pore air bubbles entrapped within the structure of gelled substance and allowed the air to respond so as to increase the compressibility as a whole. On the other hand, the soil specimens of the test series A, C and D were found to contain only dispersed air attached to the structure of gelled substance and the air did not contribute to the change in the V_p-value. Particularly in the test series D, there are two different types of response of the gelled substance as

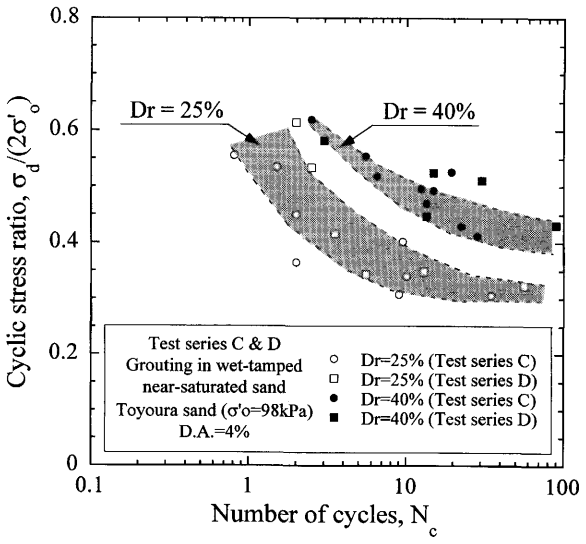

Fig. 18. Plots of cyclic stress ratio against number of cycles in test series C and D

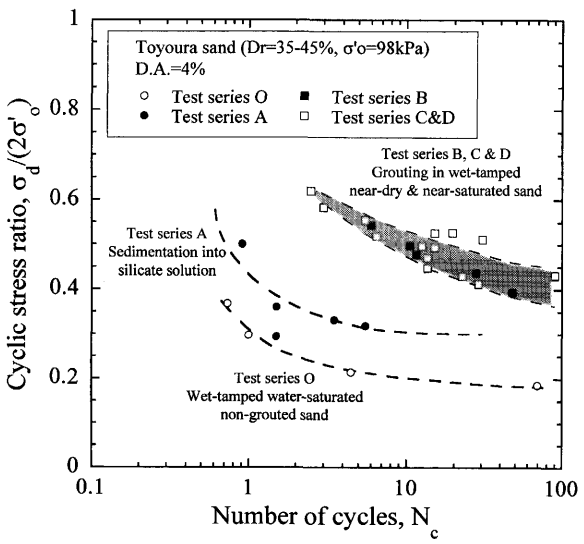

Fig. 20. Summary plots of cyclic stress ratio against number of cycles (D_r = 35–45%)

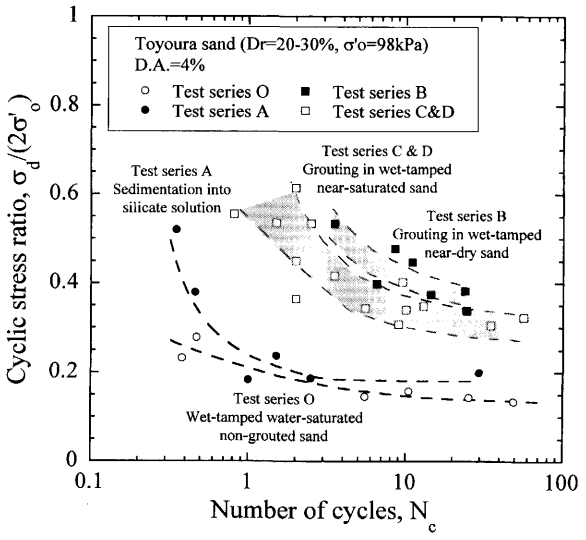

Fig. 19. Summary plots of cyclic stress ratio against number of cycles (D_r = 20–30%)

described above, presumably induced by the sustained application of an overburden stress during the curing period, which resulted in the fractured or non-fractured structures of gelled substance. With this fact in mind, it would be of interest to examine whether these differences in the non-destructive tests are reflected in the cyclic phase of loading which is destructive in nature.

The comparisons of the data in this context for all the test series with the relative density of D_r = 25% are shown in Fig. 19. Since it is known that the method of sample preparation affects the cyclic resistance of soils due primarily to different structures of soil fabric, it would be preferable to compare the results of grouted and non-grouted sand specimens prepared by the same method. However, the results of non-grouted sand specimens prepared by the method of wet tamping are only available in the present study. The cyclic stress ratios for the specimens prepared by the method of the silicate-solution sedimentation are seen being slightly greater than that of the wet-tamped non-grouted saturated sand at any number of cycles, N_c. Grouting on the wet-tamped specimens in the test series B, C and D gives the cyclic stress ratios twice as great as that of the wet-tamped non-grouted saturated sand. In particular, the inclusion of pore air bubbles within voids formed by grouting on nearly dry sand in the test series B, makes the soil specimens somewhat more resistant and leads to the cyclic stress ratios which are greater than that of the grouted saturated sand in the test series C and D. However, there is no discernable difference among the data of the test series C and D. Therefore, it may be mentioned that there is negligible influence of the sustained application of an overburden stress applied during the curing period on the cyclic resistance, no matter whether the gelled substance in the sample was of fractured or non-fractured type. The comparison in the same vein is shown in Fig. 20 for the samples with the relative density of D_r = 40%. For the dense sand specimens, the difference as above disappears and there are no significant differences in the cyclic stress ratios among the test series B, C and D, regardless of whether grouting or permeation was conducted on nearly dry sand or saturated sand.

In looking at the test data shown in Figs. 16 to 20, the cyclic strength is defined as, $\sigma_{d,\ell}/(2\sigma'_o)$, which is the cyclic stress ratio causing 4% DA axial strain in the course of 20 cycles of load application. The cyclic strength thus defined is now plotted against the relative density, as shown in Fig. 21. Overall, it is found that at any value of the relative density, the specimens prepared by the method of sedimentation (test series A) exhibited the cyclic resistance twice as large as that of non-grouted saturated sand (test series O). In the case of the wet-damped grouted specimens (test series B, C and D), the cyclic resistance was three times larger than that of non-grouted saturated sand.

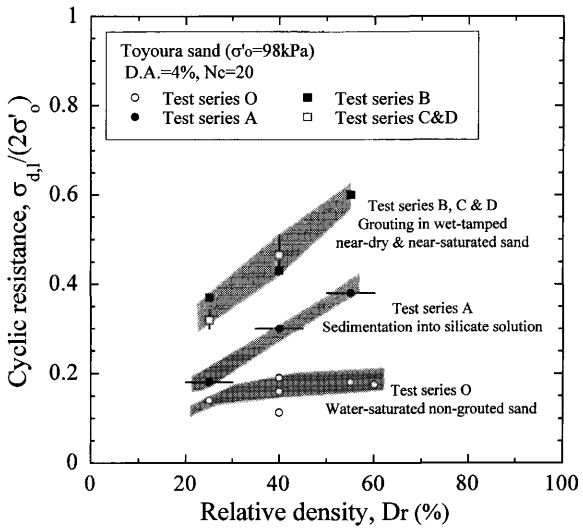

Fig. 21. Plots of cyclic resistance against relative density

CONCLUSIONS

Using the triaxial test apparatus, two phases of tests were conducted on variously prepared sand samples, i.e., non-destructive wave propagation tests and destructive cyclic loading tests. A group of sand samples was prepared in the condition saturated with water. The second group of samples was formed by sedimentation of sand into silicate solution. The third group was prepared by wet tamping of silicate-mixed sand. The fourth group was prepared by the method of wet tamping of silicate-mixed sand, but subjected to an effective overburden pressure during the curing period. The results of the test show that, while the shear wave velocity is not affected so much, the longitudinal wave velocity is influenced significantly by the *B*-value and also by the method in which the specimens were prepared.

In the phase of the destructive tests, the specimens prepared by the method of sedimentation into silicate solution showed the cyclic resistance about 1.1 times as much as that of non-grouted saturated sand. Grouting on nearly dry sand seems to produce specimens containing a sufficient amount of air bubbles trapped within the structures of gelled substances. Such samples exhibited the cyclic strength about 2.5 times greater than that of the non-grouted samples. Grouting on saturated sand appears to produce soil specimens containing partly saturated water within the structure of gelled substance and such specimens showed the cyclic resistance, which is about twice greater than that of non-grouted saturated sand. On the other hand, the sustained application of an overburden stress over the curing period of one month did not exhibit significant influence on the cyclic strength.

ACKNOWLEDGEMENTS

The authors would like to express their sincere appreciation to the past students of Tokyo University of Science, M. Shimane and J. Sato for their cooperation in conducting the laboratory tests reported in the present paper. Thanks are also extended to Mr. A. Yoshida and Mr. T. Hada of Raito Kogyo Co., for their generous support on the present study. This research was funded by Ministry of Education, Science and Technology.

NOTATION

B: *B*-value
G_o: initial shear modulus
N_c: number of cycles in undrained cyclic triaxial tests
V_p: velocity of propagation of longitudinal wave
V_s: velocity of propagation of shear wave
ε_a: axial strain
σ'_o: effective confining stress
σ_d: amplitude of cyclic axial stress
$\sigma_{d,\ell}/(2\sigma'_o)$: cyclic resistance, defined as the cyclic stress ratio at 4% D.A. axial strain and $N_c = 20$
ν: overall Poisson's ratio
ν_b: skeleton Poisson's ratio

REFERENCES

1) Hatanaka, M., Uchida, A., Matsumura, M. and Imazato, T. (2002): Evaluation of chemical grouted area by resistivity tomography method, *Soils and Foundations*, **42**(4), 69–75.
2) Ishihara, K. and Tsukamoto, Y. (2004): Cyclic strength of imperfectly saturated sands and analysis of liquefaction, *Proc. Jpn. Academy*, Ser.B, **80**(8), 372–391.
3) Ishihara, K., Tsukamoto,Y. and Kamada, K. (2004): Undrained behaviour of near-saturated sand in cyclic and monotonic loading, *Proc. Int. Conf. Cyclic Behaviour of Soils and Liquefaction Phenomena*, Bochum, Germany, 31 March–02 April 2004; Cyclic Behaviour of Soils and Liquefaction Phenomena (ed. by Triantafyllidis, Th.), Taylor & Francis Group, London, 27–39.
4) Japanese Geotechnical Society (1993): Prediction and evaluation of performance of chemical grouting, *Technical Committee Report*, 1–144 (in Japanese).
5) Kaga, M. and Yonekura, R. (1991): Estimation of strength of silicate-grouted sand, *Soils and Foundations*, **31**(3), 43–59.
6) Kokusho, T. (2000): Correlation of pore-pressure *B*-value with P-wave velocity and Poisson's ratio for imperfectly saturated sand or gravel, *Soils and Foundations*, **40**(4), 95–102.
7) Mori, A. and Tamura, M. (1986): Effect of dilatancy on permeability in sands stabilized by chemical grout, *Soils and Foundations*, **26**(1), 96–104.
8) Mori, A., Tamura, M. and Fukui, Y. (1989): Distribution of grouts in solidified region on chemical grouting, *Soils and Foundations*, **29**(4), 127–134.
9) Nakazawa, H., Ishihara, K., Tsukamoto, Y. and Kamata, T. (2004): Case studies on evaluation of liquefaction resistance of imperfectly saturated soil deposits, *Proc. Int. Conf. Cyclic Behaviour of Soils and Liquefaction Phenomena*, Bochum, Germany, 31 March–02 April 2004; Cyclic Behaviour of Soils and Liquefaction Phenomena (ed. by Triantafyllidis, Th.), Taylor & Francis Group, London, 295–304.
10) Tsukamoto, Y., Ishihara, K., Nakazawa, H., Kamada, K. and Huang, Y. (2002): Resistance of partly saturated sand to liquefaction with reference to longitudinal and shear wave velocities, *Soils and Foundations*, **42**(6), 93–104.